

LOW POWER UWB CMOS RADAR SENSORS

ANALOG CIRCUITS AND SIGNAL PROCESSING SERIES

Consulting Editor: Mohammed Ismail, Ohio State University

Titles in Series:

- LOW POWER UWB CMOS RADAR SENSORS**
Paulino, Nuno, Goes, João, Steiger Garção, Adolfo
ISBN: 978-1-4020-8409-6
- THE GM/ID DESIGN METHODOLOGY FOR CMOS ANALOG LOW POWER INTEGRATED CIRCUITS**
Jespers, Paul G.A.
ISBN-10: 0-387-47100-6
- SUBSTRATE NOISE COUPLING IN RFICS**
Helmy, Ahmed, Ismail, Mohammed
ISBN: 978-1-4020-8165-1
- CIRCUIT AND INTERCONNECT DESIGN FOR HIGH BIT-RATE APPLICATIONS**
Veenstra, Hugo, Long, John R.
ISBN: 978-1-4020-6882-9
- HIGH-RESOLUTION IF-TO-BASEBAND SIGMADELTA ADC FOR CAR RADIOS**
Silva, Paulo G.R., Huijsing, Johan H.
ISBN: 978-1-4020-8163-7
- MULTI-BAND RF FRONT-ENDS WITH ADAPTIVE IMAGE REJECTION
A DECT/BLUETOOTH CASE STUDY**
Vidojkovic, V., van der Tang, J., Leeuwenburgh, A., van Roermund, A.H.M.
ISBN: 978-1-4020-6533-0
- SILICON-BASED RF FRONT-ENDS FOR ULTRA WIDEBAND RADIOS**
Safarian, Aminghasem, Heydari, Payam
ISBN: 978-1-4020-6721-1
- DESIGN OF HIGH VOLTAGE XDSL LINE DRIVERS IN STANDARD CMOS**
Serneels, Bert, Steyaert, Michiel
ISBN: 978-1-4020-6789-1
- BASEBAND ANALOG CIRCUITS FOR SOFTWARE DEFINED RADIO**
Giannini, Vito, Craninckx, Jan, Baschiroto, Andrea
ISBN: 978-1-4020-6537-8
- HIGH-LEVEL MODELING AND SYNTHESIS OF ANALOG INTEGRATED SYSTEMS**
Martens, Ewout S.J., Gielen, Georges
ISBN: 978-1-4020-6801-0
- CMOS MULTI-CHANNEL SINGLE-CHIP RECEIVERS FOR MULTI-GIGABIT OPT...**
Muller, P., Leblebici, Y.
ISBN 978-1-4020-5911-7
- ANALOG-BASEBAND ARCHITECTURES AND CIRCUITS
FOR MULTISTANDARD AND LOW-VOLTAGE WIRELESS TRANSCEIVERS**
Mak, Pui In, U, Seng-Pan, Martins, Rui Paulo
ISBN: 978-1-4020-6432-6
- FULL-CHIP NANOMETER ROUTING TECHNIQUES**
Ho, Tsung-Yi, Chang, Yao-Wen, Chen, Sao-Jie
ISBN: 978-1-4020-6194-3
- ANALOG CIRCUIT DESIGN TECHNIQUES AT 0.5V**
Chatterjee, S., Kinget, P., Tsvividis, Y., Pun, K.P.
ISBN-10: 0-387-69953-8
- SWITCHED-CAPACITOR TECHNIQUES FOR HIGH-ACCURACY FILTER AND ADC...**
Quinn, P.J., Roermund, A.H.M.v.
ISBN 978-1-4020-6257-5
- LOW-FREQUENCY NOISE IN ADVANCED MOS DEVICES**
von Haartman, M., Östling, M.
ISBN 978-1-4020-5909-4
- ULTRA LOW POWER CAPACITIVE SENSOR INTERFACES**
Bracke, W., Puers, R. (et al.)
ISBN 978-1-4020-6231-5
- BROADBAND OPTO-ELECTRICAL RECEIVERS IN STANDARD CMOS**
Hermans, C., Steyaert, M.
ISBN 978-1-4020-6221-6
- CMOS SINGLE CHIP FAST FREQUENCY HOPPING SYNTHESIZERS FOR WIRELESS
MULTI-GIGAHERTZ APPLICATIONS**
Bourdi, Taoufik, Kale, Izzet
ISBN: 978-1-4020-5927-8
- CMOS CURRENT-MODE CIRCUITS FOR DATA COMMUNICATIONS**
Yuan, Fei
ISBN: 0-387-29758-8

LOW POWER UWB CMOS RADAR SENSORS

by

Nuno Paulino, João Goes and Adolfo Steiger Garção

*Universidade Nova de Lisboa, Fac. Ciências e Tecnologia, Depto. Engenharia
Electronica, Quinta da Torre, 2825-114 Caparica, Portugal*

 Springer

Nuno Paulino
Universidade Nova de Lisboa
Fac. Ciências e Tecnologia
Depto. Engenharia Electronica
Quinta da Torre
2825-114 Caparica
Portugal
nunop@uninova.pt

João Goes
Universidade Nova de Lisboa
Fac. Ciências e Tecnologia
Depto. Engenharia Electronica
Quinta da Torre
2825-114 Caparica
Portugal
jg@uninova.pt

Adolfo Steiger Garção
Universidade Nova de Lisboa
Fac. Ciências e Tecnologia
Depto. Engenharia Electronica
Quinta da Torre
2825-114 Caparica
Portugal

ISBN 978-1-4020-8409-6

e-ISBN 978-1-4020-8410-2

Library of Congress Control Number: 2008925809

© 2008 Springer Science+Business Media B.V.

No part of this work may be reproduced, stored in a retrieval system, or transmitted in any form or by any means, electronic, mechanical, photocopying, microfilming, recording or otherwise, without written permission from the Publisher, with the exception of any material supplied specifically for the purpose of being entered and executed on a computer system, for exclusive use by the purchaser of the work.

Printed on acid-free paper

9 8 7 6 5 4 3 2 1

springer.com

List of Abbreviations and Acronyms

ADC	Analog to Digital Converter
AGC	Automatic Gain Control.
CMOS	Complementary MOS
CP	Charge Pump
DAC	Digital to Analog Converter
DC	Direct Current
DLL	Delay Locked Loop
DSP	Digital Signal Processor
DTC	Digital to Time Converter
EIRP	Effective Isotropic Radiated Power
ESD	Electro-Static Discharge
FCC	Federal Communications Commission.
FFT	Fast Fourier Transform
FIB	Focused Ion Beam
GaAs	Gallium Arsenide
GBW	Gain Bandwidth product
GPR	Ground Penetrating Radar
IC	Integrated Circuit
IF	Intermediate Frequency
IFFT	Inverse FFT
JLCC	Ceramic Leaded Chip Carrier (J Lead)
LC	inductor-Capacitor circuit
LNA	Low Noise Amplifier
lsb	least significant bit
MiM	Metal isolator Metal capacitor
MOS	Metal Oxide Semiconductor
NF	Noise Figure
NMOS	N channel MOS transistor
PCB	Printed Circuit Board
PD	Phase Detector
PLL	Phase Locked Loop
PMOS	P channel MOS transistor
PRF	Pulse Repetition Frequency
PRI	Pulse Repetition Interval
PSD	Power Spectral Density
RADAR	RAdio Detection And Ranging
RC	Resistor-Capacitor circuit
RF	Radio Frequency
RLC	Resistor-inductor-Capacitor circuit
rms	root mean square

vi List of Abbreviations and Acronyms

SAW	Surface Acoustic Wave
$\Sigma\Delta$	Sigma Delta modulator
S&H	Sample and Hold
sinc	$\sin(x)/x$ function
SMD	Surface Mounted Device
SNR	Signal to Noise Ratio
TDR	Time Domain Reflectometry
UWB	Ultra Wide Band
VCDL	Voltage Controlled Delay Line

Contents

1	Introduction	1
2	UWB Signals and Systems	5
2.1	A Brief History of UWB Systems and their Applications	5
2.2	Spectrum and Power of UWB Signals	17
2.3	Antennas for UWB Signals.....	26
2.3.1	Electrically Small Antennas	30
2.3.2	Resonant Antennas	34
2.3.3	Broadband Antennas	37
2.3.4	Aperture Antennas.....	43
2.3.5	Antenna Summary	44
	References	45
3	UWB RADAR Receiver Architecture.....	49
3.1	UWB RADAR Systems.....	49
3.2	UWB Radar Equation.....	54
3.3	UWB Receiver Architecture.....	62
3.3.1	The Sub-Sampling Technique	62
3.3.2	The Problem of Generating the Sampling Clock.....	64
3.3.3	Using a Programmable Delay	65
3.3.4	The Sample and Hold	67
3.3.5	Averaging Samples Together	73
3.3.6	Using a Low Noise Amplifier	77
3.3.7	Using a Switched-Integrator.....	85
3.3.8	Differential Switched-Integrator Circuit	95
3.3.9	Offset Calibration	102
3.3.10	Differential Switched Integrator Noise Analysis.....	108
3.4	Receiver Specifications	111
	References	113
4	Digitally Programmable Delay	115
4.1	Architecture	116
4.2	High Level Analysis and Design	118
4.3	Electrical Design.....	129
4.3.1	Differential Buffer.....	129
4.3.2	Replica Bias Circuit.....	143
4.3.3	Voltage Controlled Delay Line.....	148
4.3.4	Phase Detector.....	153
4.3.5	Charge Pump Architecture and Design	156
4.3.6	DLL Auxiliary Circuits	164
	References	165

- 5 Transceiver Prototype and Experimental Results..... 167**
 - 5.1 Transceiver Circuit 167
 - 5.1.1 Short Pulse Generator 169
 - 5.1.2 Receiver Channel..... 174
 - 5.1.3 Prototype Integrated Circuit 186
 - 5.2 Experimental Results 190
 - 5.2.1 Short Pulse Generator 194
 - 5.2.2 Switched-Integrator 196
 - 5.2.3 Digitally Programmable Delay 205
 - References..... 209

- 6 Conclusions 211**

- Appendix A Echo Signals from Moving Targets 215**

- Appendix B Gain and Offset Errors in the S&H Due to the MOS Switches..... 219**

- Appendix C Sigma Delta Modulator 223**

- Appendix D Bond-Wire Parasitic Effects..... 229**

- Appendix E Oscilloscope Characterization..... 231**

- Index 235**

Chapter 1

Introduction

The objective of the work presented in this book is the study, design and implementation of a low-cost, low-power radar sensor, using CMOS technology. This radar sensor can have several applications, including:

- *Proximity sensor*: being able to detect any intruders that enter a safety perimeter, defined around the sensor.
- *Motion detector*: being able to detect motion of objects around the sensor.
- *Ground penetrating radar*: Since the radar sensor will use signals with a large bandwidth at low frequency, it will be capable of detecting artifacts buried at shallow depth in some types of soil.
- *2D/3D imaging*: by combining the outputs of several radar sensors and using signal processing techniques it is possible to obtain a 2D/3D image.

The operation principle of a radar system is very simple: an electromagnetic signal (pulse) is radiated, this signal travels at the speed of light (assuming that the signal propagates in space), when the signal encounters an object part of its energy is re-radiated therefore creating an echo, the echo signal travels back to the point of radiation of the original signal at the speed of light. This signal can be detected and the time interval between the transmission of the signal and arrival of the echo can be measured. The capability of the radar to distinguish between two targets close to each other is dependent on the relation between the pulse width and the time it takes for the light to travel the distance between the two targets. If the pulse width is larger than this time, it is very difficult to distinguish the echoes from each target. In order to separate two targets placed close together it is important to use a small pulse width. The bandwidth of signal with a given time duration (pulse) is approximately equal to the inverse of the signal time duration. If a pulse signal is used to modulate a sine-wave carrier, the resulting signal will have approximately the same bandwidth as the pulse signal centered around the carrier frequency. So, if traditional narrow band signals are used, the carrier frequency needs to be very high, in order to obtain a relatively low fractional bandwidth. This high frequency would result in the need for expensive RF technologies such as GaAs. But if the carrier frequency is reduced, eventually using no carrier signal just the pulse signal, the resulting signal will still have the capability of resolving two targets placed close to each other. As an example if it is desired to distinguish between targets separated by a distance of 30 cm it is necessary to use a pulse width smaller than 1 ns. If this pulse is used to modulate a sine-wave signal, the carrier frequency might be as high as 20 GHz, but if the pulse is used without a carrier signal, the resulting signal will have most of its power below 2 GHz. This frequency range is within the reach of modern CMOS technologies (0.35 μm , 0.18 μm or better), which are less expensive than more exotic technologies.

A signal which has a very large bandwidth compared to its center frequency value is known as an UWB signal and it has been known and utilized since the end of the nineteenth century. The interest in these types of signals has increased in the last years due to the potential benefits of imaging and communications systems based on UWB signals. Although initially, the use of UWB signals was prohibited because these signals would interfere with narrow band RF signals, recently it was realized that if the power of the UWB signal is low, the interference is limited and UWB signals can share the same electromagnetic spectrum as narrow band RF signals. This allows using the same electromagnetic spectrum (which a scarce resource) for different applications. In 2002 the FCC recognized this and allowed to use UWB signals in a variety of applications, as long as the PSD of the signals was limited to certain levels. UWB systems radiate signals with very low power level, to reduce the interference with narrow band systems. This means that the range of operation for UWB systems will be short; however by exploring the high bandwidth of UWB signals it is possible to obtain high data rate digital communications at short ranges or creating high-resolution radar images.

This book is divided in 6 chapters; a brief overview of the following chapters is given next.

The second chapter introduces UWB signals and systems. The utilization of UWB systems, in the last one hundred years, is described in a brief history of UWB signals and systems, showing that this type of signals were used in the beginning of the radio history, but were abandoned in favor of narrow band RF signals. During a long time UWB signals survived in niche applications. However, in the last 15 years, the evolution of the CMOS technology enabled a reduction of the cost of UWB systems and, at the same time, enabled an expansion of their functionality. This led to a renovated interest in UWB systems, both for communications and for imaging applications. This chapter shows some examples of UWB signals and characterizes the time domain and frequency domain properties of these signals. It is shown, that baseband UWB signals can be easily generated using circuits built in a CMOS technology, which is less expensive than more exotic technologies such as GaAs or Silicon-Germanium. The second chapter ends with a study of the interaction between UWB signals and the antennas used to transmit and receive them. In this analysis, a methodology that allows to calculate the shape of the received UWB signal in an antenna link is developed. Using this methodology, it is shown that the optimal input impedance of an UWB receiver is not necessarily the same as the optimal input impedance for a narrow band signal. There is also an analysis about the best type of antenna for UWB signals and how each type of antenna affects the PSD of the radiated signal.

The third chapter describes the operation of a radar system. The differences and advantages of using UWB signals in a radar system, over traditional narrow band signals, are discussed. The radar equation, usually defined for narrow band signals, is redefined for UWB signals. This new radar equation is used to analyze the echo signals from targets with basic shapes, resulting in an estimative of the echo signal amplitude as a function of the target distance. The architecture of an UWB radar based in the concept of sub-sampling is defined and the constituting blocks

are described. The remaining of the chapter is concentrated in analyzing the receiver channel of the radar system. This analysis is centered around the noise power level in the receive path. From this analysis a new receiver circuit for base-band UWB signals is proposed. This new circuit is an averaging switched-integrator circuit. This circuit is described in detail and a design procedure is shown.

The fourth chapter deals with the problem of generating a clock signal with a programmable delay. This clock is necessary in the radar system to define the sampling instant in the receiver channel. The delay in this clock signal is relative to the transmit clock signal and is used to determine the target distance. A new digitally programmable delay architecture that can have a large programming linearity is proposed. This architecture is based on a digital $\Sigma\Delta$ modulator that controls a 1-bit digital-to-time converter, whose output is filtered by a delay locked-loop, thus producing a delayed clock signal. This architecture is analyzed and designed, at high level, to meet the required specifications for the radar system. A high level model is used to simulate the behavior of this circuit and validate the design. The electronic sub-blocks necessary to build this circuit are described, analyzed and a design methodology for each sub-block is derived. These circuits are implemented using differential clock signals in order to reduce the noise level in the radar system.

The fifth chapter describes the experimental CMOS prototype IC that was developed to evaluate the performance of the different sub-blocks of the radar system. The first part of this chapter is dedicated to the description of the prototype IC and to the design of the short pulse generator circuit and the amplifier circuit needed in the receive path. The second part of the chapter describes the experimental evaluation of the circuit and presents the measured results for each of the radar system sub-blocks. The experimental evaluation procedures used during the testing of the prototype IC, are also described.

Finally, the sixth chapter describes an overview of the research presented in this book, draws some conclusions about obtained results and presents some suggestions for future work in this area.

Chapter 2

UWB Signals and Systems

Abstract this chapter introduces UWB signals and systems. The utilization of UWB systems, in the last one hundred years, is described in a brief history of UWB signals and systems. This chapter shows some examples of UWB signals and characterizes the time domain and frequency domain properties of these signals. It is shown, that baseband UWB signals can be easily generated using circuits built in a CMOS technology. The chapter ends with a study of the interaction between UWB signals and the antennas used to transmit and receive them. In this analysis, a methodology that allows to calculate the shape of the received UWB signal in an antenna link is developed. Using this methodology, it is show that the optimal input impedance of an UWB receiver is not necessarily the same as the optimal input impedance for a narrow band signal. There is also an analysis about the best type of antenna for UWB signals and how each type of antenna affected the PSD of the radiated signal.

2.1 A Brief History of UWB Systems and their Applications

The first intentional emission of electromagnetic radiation was based in the generation of electrical signals with short duration [1]. In his pioneering experiments, Heinrich Hertz [2] invented a RF oscillator consisting of a resonant circuit (a balanced half wave length dipole, capacitively loaded by large metal spheres) and a fast acting switch (a spark gap in the center of the dipole). This arrangement was operated by applying a high voltage DC pulse to the dipole, this high voltage DC pulse was generated by the secondary of a transformer where a large DC current (i_1) was interrupted in the primary. A simplified representation of this circuit is shown in Fig. 2.1.

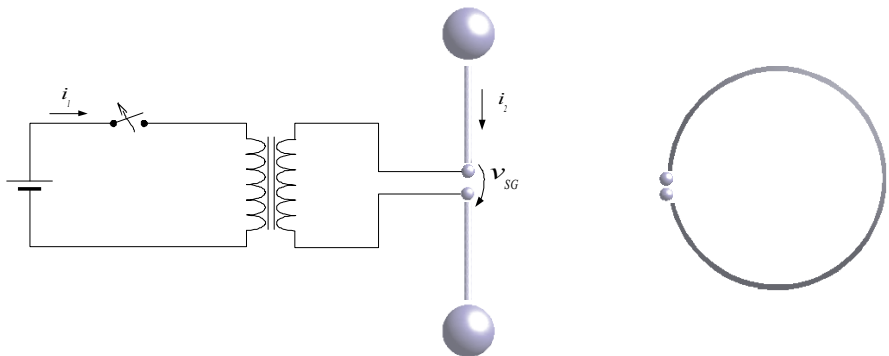


Fig. 2.1 Simplified representations of the Hertz RF generator and receiver

The capacitance of the dipole is charged by the high voltage pulse until the voltage across the spark gap (v_{SG}) is enough to cause a spark. The spark arc has a low resistance that effectively connects the two parts of the dipole causing a large abrupt current (i_2) to flow between the two charged spheres. This current causes a magnetic field that reaches its maximum value when the electrical field between the two spheres is zero. As the magnetic field collapses, the electrical field increases (with an opposite polarity as before) because the current continues to flow charging the spheres, when the current reaches zero, the energy is once again stored in the electrical field and the cycle will repeat itself. The charge will thus flow back and forth between the spheres, as the energy alternates between the magnetic and the electrical field, except that approximately 15% of the energy is radiated as RF energy in each half cycle. The dipole produces about five half-cycles of RF energy for each high voltage pulse applied. The typical output wave of this oscillator is a short duration damped sine-wave and the resulting RF frequency spectrum is very wide.

In his experiments Hertz used his oscillator apparatus to generate electromagnetic waves with frequencies¹ of 50 MHz, 100 MHz and 430 MHz; he used such high frequencies in order to obtain a wave-length with an acceptable small value, necessary to run his experiments inside his laboratory. He detected the electromagnetic waves using a very small spark gap connected to a resonant circuit consisting of a loop with half wave-length (as shown in Fig. 2.1). A small spark would indicate the presence of an electromagnetic field; this setup is not very sensitive and requires almost complete darkness to detect the small spark. Nevertheless, he was able to measure the wave length by determining the position of the peaks and nulls of the radiated RF signal.

Latter Marconi used and perfected Hertz experiments in order to obtain a wireless telegraphy system. His systems used variable capacitors to provide tuning to both receivers and transmitters, in order to select different frequencies of operation [3]. The transmitters were still based in spark plugs and therefore a considerable amount of RF energy was spread outside the band of interest, resulting in inefficient operation. The receivers were based on coherer tubes, a glass tube filled with metallic powder, whose resistance would drop approximately an order of magnitude when submitted to an electrical discharge. The sensitivity of this detector is very low. These systems were suited for communication using only Morse code. To compensate the large inefficiencies of the transmitters and of the receivers, the transmitters needed to radiate a large amount of power (over 10 kW). The result was, as the number of spark plug transmitters increased, the interference between them prevented clear communication between a given transmitter and a given receiver. This led to the invention and development of continuous wave oscillators, where the output signal is a continuous sine wave with a desired frequency value, resulting in a reduction of the power transmitted outside the desired frequency band and therefore a reduction in the interference between different transmitters.

¹ This is the fundamental frequency of the damped sine-wave pulse which is very rich in harmonics.

The sensitivity of the receiver circuits was improved, with the discovery of the first asymmetrical electrical junctions, such as the point contact crystal detector, which also improved the range and quality of the communication channel. The invention of the vacuum tube by DeForest in 1906 led to new circuits [4], [5], such as the superheterodyne receiver (invented by Edwin Armstrong around 1917) [6], which has an excellent frequency discrimination capability and sensitivity (this radio architecture is still the base for most of the radios used today). As a result, gradually the spark plug transmitters were abandoned and finally prohibited in 1927, since their large spectrum usage would interfere with narrow band RF systems.

Interest in radio systems based on short pulses never disappeared, during the 1940's several patents were issued for systems using short pulses such as the patent for a "Random Impulse System" issued in 1942 (US patent 2671896), but no practical applications for these systems existed. The practical use of non-sinusoidal RF signals reappeared in the 1960's with the objective of analyzing the properties of distributed microwave networks, first as an analytical tool but latter, with the development of synthetic generators and sampling oscilloscopes, these signals, called baseband pulses or carrierless pulses, were used to experimentally determine the intrinsic properties of materials and distributed networks [7], [8], by analyzing the reflections created by the input pulses, this type of analysis is know as Time Domain Reflectometry (TDR).

The synthetic generator consisted of a distributed pulse forming network, where a step function (created by a tunnel diode source) with sub-nanosecond rising time was applied. The pulse forming network had open and short circuit stubs located at precise distances in order to transform the incident step to a rectangular pulse and by appropriately inverting, recombining and filtering these pulses, into an output consisting of several RF cycles [8], [9].

The sampling oscilloscope uses equivalent time sampling to acquire signals whose bandwidth exceed half of the maximum sample rate of the oscilloscope [10]. The input signal is applied directly to a sampling bridge and is sampled before any attenuation or amplification is performed. The attenuator or amplifier circuits are placed after the signal has been converted to a lower frequency by the sampling circuit, and can have a lower bandwidth than the input signal. Therefore the sampling oscilloscope can have an input bandwidth much larger than the sample rate. The equivalent time sampling takes advantage of the fact that most man made events can be repetitive. Equivalent time sampling constructs an image of a fast repetitive signal by sampling a point of the input signal in each repetition. Each time, a different point is sampled and after a certain time it is possible to reconstruct the shape of the fast input signal. This principle, known as sub-sampling, is illustrated in Fig. 2.2 This process allows a sampling oscilloscope to display signals whose frequency components are much higher than the oscilloscope sample rate (but inferior to the sampling bridge input bandwidth).

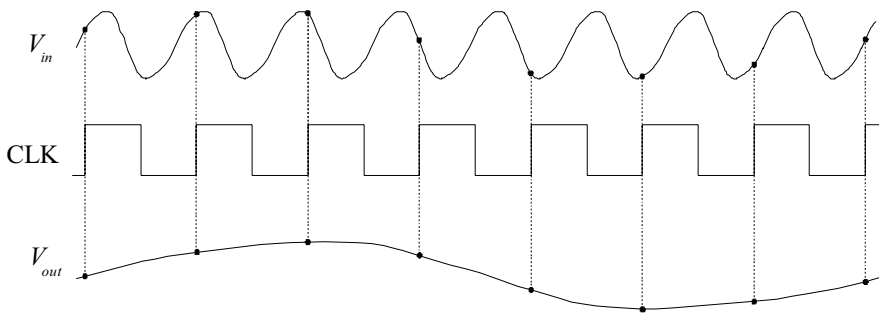


Fig. 2.2 Sub-Sampling of a repetitive fast input signal in order to produce a slow output signal with the same shape as the fast input signal

Using pulses with very short duration it is possible to measure the impulse response (through a sampling oscilloscope) of a distributed microwave network and then calculate the frequency response using the Fourier transform. The maximum and minimum frequency values of the analysis are determined by the pulse width (the shorter the pulse the higher the maximum frequency value of the analysis) and by the duration of the observation time (the longer the observation time the lower the minimum frequency value of the analysis). Of course that increasing the maximum and the minimum frequency of the analysis requires both a fast sampling frequency in the oscilloscope and a large number of sampled points of the impulse response. This procedure reduced the time needed to measure the frequency domain properties of radar stealthy materials by a factor of 100 [8]. The traditional method consists in applying a sine-wave signal, measuring the S parameters and then repeating the procedure for the different frequencies of interest. This is the method of choice for narrow band systems. But for wide band systems, such as today's digital systems (Rambus, USB 2.0, Firewire and others), it is difficult to interpret the measured frequency response and understand where the discontinuities in the transmission lines are physically located. TDR provides a more intuitive and direct look into the signal integrity in digital systems [11], [12]. By using a step generator to generate a fast edge into the transmission line and using a sampling oscilloscope to monitor the reflected waves at different points in the line it is possible to locate the line discontinuities and understand the nature (resistive, inductive or capacitive) of each discontinuity. It is also possible to understand whether losses in a transmission system (a circuit board trace, a cable, a connector and so on) are series losses or shunt losses.

TDR has also been used to locate various defects in electrical power distribution cables (such as: voids, shield protrusions, contaminants, etc.) by locating partial discharge events in the cable [13], [14]. The cable under test, terminated with an open end, is connected to an excitation voltage source at the other end. This voltage is gradually increased until a partial discharge (PD) event occurs at a certain point in the cable; the pulses generated by the PD event travel in the cable and are reflected by the ends of the cable until they disappear because of the cable

attenuation. By measuring the time between the arrivals of the various pulses at one end of the cable it is possible to determine where the defects are located.

Another area of application for TDR techniques is liquid level measurement in tanks [15], [16]. The level of the liquid (or liquids) in a tank can be determined using a probe line that acts as an open transmission line for the TDR pulse signal. The tank contents that surround the probe line become the transmission line isolating dielectric. At each fluid interface, a change in the dielectric constant of the fluid surrounding the probe results in a change in the electrical impedance of the line that reflects a portion of the input pulse amplitude to the TDR receiver. The Pulse reflection amplitude and timing information can be used to accurately determine the fluids levels and the location of each fluid interface within the tank (if more than one type of fluid is present in the tank).

In the 1970's it became apparent that the sub-nanosecond pulse technology could be employed in a variety of proximal sensing applications [8], [17], this is essentially extending the time domain reflectometry principles to work in free space without a transmission line, this is also know as free-space time-domain reflectometry. Since in those systems, the objective is simply to determine the presence or absence of a return signal from a possible target, the return sensing system (receiver) can be designed to determine the threshold (location) information only, leading to significant reductions in cost and complexity of the required electronics for target signature analysis. The receiver senses, over a narrow time window, when the input signal exceeds a given threshold value, indicating the presence of a target and determines the time delay between this event and the initial transmission of the sub-nanosecond pulse. The distance to the target is directly related to this time delay. This type of systems can be used to establish security "bubbles", where an alarm is triggered if something enters the protected area. In [8] two types of receivers are described. The first, called single-hit receiver is based on a tunnel diode that is triggered by the input very-fast low energy impulse. This receiver is depicted in Fig. 2.3.

circuit is ready to detect another fast pulse at the input. In conclusion this circuit works as a monostable circuit, that when a small amplitude short pulse is presented to its input, produces a large amplitude pulse with a long duration at the output. This output pulse can be used to measure the time between the transmitted pulse and the return pulse created by the target (echo) and therefore, determine the distance of the target. The clock signal that triggers the transmission of the short pulse can be applied to a transmission line with the necessary time delay for the pulse to travel to target and back to the receiver; this delayed clock can be used to sample the output of the receiver, to determine if a target is present at the predetermined distance. The sensitivity of this receiver is determined by the tunnel diode, if this device is biased closer to its turning point, the amplitude value of the input pulse necessary to trigger the diode is reduced. This means that the circuit threshold has been lowered and it will be more sensitive to any input pulses, but at the same time it will be more prone to trigger on unwanted signals, i.e. circuit noise.

The second type of receiver described in [8], called a constant false-alarm rate receiver, improves the sensibility of the single-hit receiver by processing several hits before signaling the detection of the target. The receiver is essentially the same, except that the bias current of the tunnel diode is adjusted by a feedback loop. The objective is to bias the diode as close as possible to the threshold of the negative resistance region, to increase the sensitivity of the receiver. The feedback loop is controlled by the number of hits detected when no signal is present. This is archived by radiating the pulse on the rising edge of a clock and sampling the output of the single-hit receiver on the falling edge of the clock. As the sensitivity of the receiver is increased the number of false hits increases, the feedback loop will adjust the bias current of the tunnel diode until the number of false hits is equal to 3 over 32 observation time instants. This means that the probability of a false hit is around $(1/16)$, the probability of 32 consecutive false hits would be equal to $(1/16)^{32}$ which is a very small number. The output of the single hit receiver is sampled when the clock is present and the number of hits obtained is added, a target is considered to be present when this sum exceeds 25, this will eliminate most of the false hits. A proximity radar for detecting incoming ammunitions, using this receiver, is described in [18].

In the early 1990's, McEwan [19] developed a low cost, low power impulse radar system, using discrete components mounted on a small PCB; this sensor is called Micropower Impulse Radar (MIR). This radar sensor uses impulses with a duration between 1 and 2 ns. These pulses are generated by applying a step signal to a step recovery diode. The radar transmitter emits these pulses with a random interval to reduce the probability of interference between different radar sensors. Each sensor has a random noise generator that modulates the period of the square wave that is used to generate the short pulses. A simple block diagram of the impulse transmitter is shown in Fig. 2.4

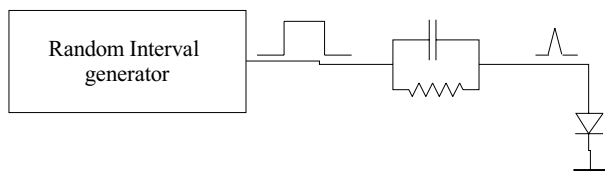


Fig. 2.4 Block diagram of the impulse transmitter used by the MIR radar sensor

The short pulses are generated using a step recovery diode [20]. Normal diodes have a slow transition when the current is switched from forward to backward, the step diode is designed to have an abrupt transition when the switch occurs, thus producing a short pulse.

The pulse transmitter has nominal pulse repetition interval (PRI) typically equal to $1 \mu\text{s}$, meaning that on average 1 million impulses per second are radiated. The receiver is constituted by two single ended integrating samplers. These circuits are constituted by a diode switch followed by an analog integrator. This integrator averages the input samples, if no signal is present the average output of the integrators will not change, if a signal is present the average output of the integrator will increase. This configuration integrates several impulses to improve the circuit sensitivity, taking advantage of the large number of available impulses. The input signal is sampled into an integrating capacitor when a strobe signal is applied. This strobe signal is generated from the random interval generator using a circuit equal to the one depicted in Fig. 2.4. The strobe signal determines the range at which a target might be located, thus a delay must be inserted between the random interval generator and the short pulse generator circuit. In a simple application, such as intrusion detection this delay can be constant and its value determines the value of the security perimeter.

Another area where UWB signals have been applied is the field of subsurface radar. The objective is to detect and locate buried artifacts and structures within the upper regions of the earth's surface [21], [22]. Any dielectric variation in the buried materials, produces a reflection from an incoming electromagnetic signal, this reflection can be used to determine the depth and type of buried material. Since the materials that constitute the earth structure introduce a high signal attenuation, the maximum operating depth of these radars is usually limited to a few meters (the signal attenuation ranges from 10 dB per meter to 200 dB per meter, depending on the material). The signal attenuation is dependent on the type of materials of the soil and, in general, it increases with the signal frequency. The maximum useful frequency is below 1 GHz, for example wet clay soil has an attenuation of 30 dB per meter for a frequency value of 100 MHz and an attenuation of 100 dB per meter for a frequency value of 1 GHz [21]. In most cases, subsurface radar systems are forced to work with signal frequencies below 1 GHz but, need to have a high-resolution to detect buried artifacts at shallow depths; therefore base-band pulses with a short duration that inherently have a large bandwidths are necessary. Typically, pulses with an amplitude of 100 V and a duration between 1 ns and 5 ns are used. The received signal is down-converted using a sampling circuit and digitized, so that complex signal processing algorithms can be applied.

Recently, UWB ground penetrating radars (GPR) have been used to detect buried mines [23], [24]. In reference [23] a GPR system using a 4 m wide array constituted by 16 UWB transmitters and 16 UWB receivers is used to build 2D and 3D images of the ground beneath the sensor. The transmitted pulses have a repetition frequency of 1 MHz and have their energy spread from 100 MHz to 3 GHz. The receivers are constituted by an RF gain stage followed by a sampler and an ADC. This type of GPR is capable of reliably detecting buried mines to a depth 50 cm.

All the previous applications show that systems using UWB signals can be as useful as narrow band systems and some of the applications are only possible using UWB systems. As a result, the use of UWB systems has been increasing over time. In the last ten years the interest in UWB systems has increased dramatically [25], this can be attributed to a simple reason: cost.

Narrow band RF systems use tuned circuits to select between different signals. These circuits are built using passive components such as inductors, capacitors or SAW filters. Until the cost of active components (transistors) started to drop exponentially (due to the constant improvement of integrated circuit technology), electronic designers minimized the number of active components in their designs to reduce cost. This is the reason why old RF systems have many passive tuned circuits that needed to be calibrated (“tuned”) before the equipment leaves the factory. As the cost of integrated circuits dropped (following Moore's Law [26]), designers started to replace passive tuned circuits by equivalent circuits using transistors, such as active filters and switched-capacitor filters. After the cost of digital signal processors (DSP) become affordable, many systems started to implement filters on DSPs (this also requires analog-to-digital and digital-to-analog converters). These techniques also reduce the need for calibration. The cost of passive components does not change much, throughout the years; the values of a capacitance, or an inductance, or a resistance, are strongly dependent on the component physical dimensions and constituting materials; therefore it is difficult to reduce its cost. On the other hand, as the cost of integrated circuits reduces (and also their size), their performance has also been doubling every 18 months. This has led to the development of electronic designs where there are less and less passive components and more advanced signal processing algorithms are used (this is even more dramatic if the ratio between the number of passive and active components is considered). A good example is the Armstrong superheterodyne receiver architecture (which is still the base for all modern radio receivers) where the last mixer is currently implemented in a DSP through the multiplication of digital signals [27]. Even the RF signals that are received are now modulated by digital signals instead of analog signals.

UWB systems do not require tuned circuits, the signals can be selected in the time domain. This makes UWB signals very amenable to digital processing techniques. These techniques can be used to improve the sensibility of UWB receivers lowering the required input RF power level, thus reducing the probability of interference with traditional narrow band systems (the main problem that plagued the first spark plug systems). Since UWB signals require a large bandwidth, it is required that the circuits processing UWB signals need to be very fast. In the past

the cost of high speed circuits was prohibitive, but, as previously stated, the cost of integrated circuit technology is dropping and the performance (speed) is increasing over time. This makes the cost of UWB systems drop over time. In the last years, there is an increasing number of proponents for the use of UWB communication systems [28], [29], [30], [31]. The objective is to use UWB signals to create short communication links (up to 10 m) with high data-rate (over 100 Mbits/sec). The required power level for the UWB signals is very low and therefore the interference between these signals and traditional narrow-band RF systems is unlikely.

In 2002 the Federal Communications Commission (FCC) [32] recognized that: “UWB technology holds great promise for a vast array of new applications that we believe will provide significant benefits for public safety, businesses and consumers. With appropriate technical standards, UWB devices can operate using the spectrum occupied by existing radio services without causing interference, thereby permitting scarce spectrum resources to be used more efficiently”. The reasoning is that since UWB devices operate using very narrow or short duration pulses that result in a very large transmission bandwidth, UWB devices can operate using spectrum occupied by existing narrow band radio services without causing interference, thereby permitting scarce spectrum resources to be used more efficiently.

UWB technology was defined as any wireless transmission device using signals whose fractional bandwidth (B_{frac}) is greater than 0.25 or occupy 1.5 GHz or more of spectrum. The formula proposed by the Commission for calculating fractional bandwidth is:

$$B_{frac} = \frac{2 \cdot (f_H - f_L)}{f_H + f_L} \quad (2.1)$$

where f_H is the upper frequency of the -10 dB emission point and f_L is the lower frequency of the -10 dB emission point. The center frequency of the transmission was defined as the average of the upper and lower -10 dB points:

$$f_c = \frac{f_H + f_L}{2} \quad (2.2)$$

Any electronic or electrical equipment always emits unwanted radiation that can interfere with narrow band radio systems. This is especially true for digital systems such as computers. Therefore every electronic and electrical device is required to limit the power of these unwanted emissions below a certain level. If UWB systems operate with power levels below the unwanted emissions level, there should not be any interference problems with other radio systems. The FCC defined three types of UWB systems: imaging systems, vehicular radar systems and communications and measurement systems. The applications and authorized operating frequency bands for these systems are defined as follows:

1. Imaging systems include Ground Penetrating Radars (GPRs), wall imaging systems, through-wall imaging systems, surveillance systems and medical imaging devices. The utilization of this type of systems is restricted to certain users (law enforcement, fire and rescue organizations, scientific research institutions, commercial mining companies and construction companies).
 - 1.1. GPRs must be operated with their -10 dB bandwidth below 960 MHz or in the frequency band 3.1–10.6 GHz. GPRs operate only when in contact with, or within close proximity of, the ground for the purpose of detecting or obtaining the images of buried objects. The energy from the GPR is intentionally directed down into the ground for this purpose.
 - 1.2. Wall-imaging systems are designed to detect the location of objects contained within a “wall,” such as a concrete structure, the side of a bridge, or the wall of a mine. Wall imaging systems must be operated with their -10 dB bandwidth below 960 MHz or in the frequency band 3.1–10.6 GHz.
 - 1.3. Through-wall Imaging Systems must be operated with their -10 dB bandwidth below 960 MHz or in the frequency band 1.99–10.6 GHz. Through-wall imaging systems detect the location or movement of persons or objects that are located on the other side of a structure such as a wall.
 - 1.4. Surveillance Systems will be permitted to operate with their -10 dB bandwidth in the frequency band 1.99–10.6 GHz. Surveillance systems operate as “security fences” by establishing a stationary RF perimeter field and detecting the intrusion of persons or objects in that field.
 - 1.5. Medical Systems must be operated with their -10 dB bandwidth in the frequency band 3.1–10.6 GHz. A medical imaging system is used to detect the location or movement of objects within the body of a person or animal.
2. Vehicular radar systems using directional antennas on terrestrial transportation vehicles provided the center frequency of the emission and the frequency at which the highest radiated emission occurs are greater than 24.075 GHz. The -10 dB bandwidth must be between 22 and 29 GHz. These devices are able to detect the location and movement of objects near a vehicle, enabling features such as near collision avoidance, improved airbag activation, and suspension systems that better respond to road conditions. Attenuation of the emissions below 24 GHz is required above the horizontal plane in order to protect space borne passive sensors operating in the 23.6–24.0 GHz band.
3. Communications and measurement systems, such as high-speed home and business networking devices as well as storage tank measurement. The devices must operate with their -10 dB bandwidth in the frequency band 3.1–10.6 GHz. The equipment must be designed to ensure that operation can only occur indoors or it must consist of hand held devices that may be employed for such activities as peer-to-peer operation. The limits on unwanted emissions are more stringent for hand held devices than they are for indoor-only systems.

The main reason for defining the above operating frequency bands for UWB systems was due to the concern of the possible interference to the GPS band at 1559–1610 MHz and the planned L5 frequency in the 960–1215 MHz band.

The specified average emission limits of the different UWB systems for the different frequency bands are given in Table 2.1. These limits are defined in terms of dBm EIRP (equivalent isotropically radiated power) as measured with a one megahertz resolution bandwidth.

Table 2.1 Average emission limits (in dBm/MHz EIRP) for UWB systems specified by the FCC

Frequency (MHz)	Indoor communication systems	Hand held communication systems	Low frequency imaging systems	Medium frequency imaging systems	High frequency imaging systems	Vehicular radar systems
<960 ³	-41.3	-41.3	-41.3	-41.3	-41.3	-41.3
960–1610	-75.3	-75.3	-65.3	-53.3	-65.3	-75.3
1610–1900	-53.3	-63.3	-53.3	-53.3	-53.3	-61.3
1900–1990	-53.3	-61.3	-51.3	-51.3	-51.3	-61.3
1990–3100	-51.3	-61.3	-51.3	-41.3	-51.3	-61.3
3100–10600	-41.3	-41.3	-51.3	-41.3	-41.3	-61.3
10600–22000	-51.3	-51.3	-51.3	-51.3	-51.3	-61.3
22000–29000	-51.3	-51.3	-51.3	-51.3	-51.3	-41.3
29000–31000	-51.3	-51.3	-51.3	-51.3	-51.3	-51.3
>31000	-51.3	-51.3	-51.3	-51.3	-51.3	-61.3

Note that -41.3 dBm/MHz corresponds to 74 nW/MHz. The total power allowed for transmission of an UWB system depends on the frequency band used by that system, the maximum power allowed for transmission (in a given frequency band) is obtained integrating the value of the EIRP from Table 2.1 over the frequency band. As an example, for an UWB system that uses the frequency band from 0 Hz to 960 MHz, the maximum power allowed is 71.2 μ W and an UWB system that uses the frequency band from 3.1 GHz to 10.6 GHz has a maximum allowed power equal to 533.7 μ W. These values correspond to the total power emitted and they

³ For frequencies below 960 MHz all UWB devices are permitted to emit at or below the part 15.209 limit of -41.3 dBm/MHz EIRP which is equivalent to an electrical field of 500 mV/m/MHz at 3 m distance.

assume that the UWB signal has a constant power spectral density value over the frequency band and has no power outside the frequency band. Normally this is not the case, the power spectral density of UWB is not constant and it is not easy to absolutely confine it to a given frequency band. These factors cause that the value of practical maximum power transmitted by an UWB system is below the previous values.

2.2 Spectrum and Power of UWB Signals

There are several signals that can be classified as UWB signals; these are typically constituted by a repetitive sequence of short pulses with a certain repetition frequency (PRF). The shape of the pulse, PRF value and the modulation (if any) determines the power spectral density (PSD) of the signal. The electromagnetic spectrum occupied by a transmitted UWB signal is determined by the PSD of the signal and by the transfer function of the antenna used to radiate the signal.

The power spectral of a periodic signal $v(t)$, $S_v(f)$, can be calculated using the Fourier series of the signals as follows [33]:

$$S_v(f) = \sum_{n=-\infty}^{+\infty} |c_n(n \cdot f_0)|^2 \cdot \delta(f - n \cdot f) \quad (2.3)$$

where f_0 is the PRF and c_n are the Fourier series coefficients given by:

$$c_n = \frac{1}{T_0} \int_{T_0} v(t) \cdot e^{-j2\pi f_0 t} dt \quad (2.4)$$

The PSD can be calculated by solving the integral (2.4) [34], [35], which can be difficult depending on the shape of the pulse and modulation, or it can be calculated numerically applying the FFT algorithm to compute the discrete time Fourier Transform of a sampled version of the UWB signal [33], [36]. Both of these approaches are valid, the PSD presented next are calculated using the FFT. Note that both of these methods result in an approximated result, since, for most pulse shapes the PSD is constituted by an infinite number of spectrum lines and the graphic representation of their PSD is always truncated. The power of the signals will be calculated considering that the signals are voltage signals, normalized to 1 V amplitude (A) and the PSD will be presented using dBV (dB to 1 V *rms*) because in order to calculate the power level in dBm, it would be necessary to know the value of the load resistance where the signal is applied. If the resistance value is known (R_L), it is easy to convert the dBV value to dBm, considering that: